ELSEVIER

Journal of Alloys and Compounds 224 (1995) 93–96

Journal of ALLOYS AND COMPOUNDS

$T(z)$ diagram and optical energy gap values of $Cu_{2(1-z)}Mn_zIn_2Te_4$ alloys

A. Rivero, M. Quintero, M. Morocoima, J.C. Woolley *

Centro de Estudios de Semiconductores, Departamento de Física, Universidad de Los Andes, Mérida, Venezuela

Received 22 August 1994; in final form 28 November 1994

Abstract

The $T(z)$ diagram of the system $Cu_{2(1-z)}Mn_zIn_2Te_4$ was obtained from X-ray powder diffraction and differential thermal analysis measurements. At high temperatures, there is single-phase solid solution across the complete diagram in a disordered defect zinc-blende phase β. This β phase shows a eutectoid reaction at $z=0.49$ and $T=452$ °C giving the two tetragonal terminal phases α, $CuInTe_2$, and γ, $MnIn_2Te_4$, of space groups $I\bar{4}2d$ and $I\bar{4}2m$, respectively. At lower temperatures, the fields α and γ are separated by a relatively wide two-phase field ($\alpha+\gamma$) which extends over the range $0.37<z<0.76$. Values of room-temperature optical energy gap E_0 were determined from optical absorption measurements in the ranges of single-phase behaviour, and the form of the E_0 vs. z data curve is discussed. The form of this $T(z)$ diagram is compared with those of related systems in which the terminal compounds have similar structure but differ in space group.

Keywords: Optical energy gap values; X-ray powder diffraction; Differential thermal analysis

1. Introduction

Semiconductor materials containing manganese are of interest because of the manner in which the magnetic behaviour associated with the manganese can modify and complement the semiconductor properties [1,2]. It has been found that adamantine compounds with tetrahedral coordination can accept a large amount of manganese in cation substitutional solid solution. Well known examples of such materials are the alloys based on the II–VI compounds, e.g. $Cd_{1-z}Mn_zTe$ [1]. Similar alloys can be obtained by introducing manganese into the equivalent ternary compounds, the tetrahedrally coordinated I–III–VI_2 chalcopyrites, e.g. $CuInTe_2$. One way of introducing Mn into these chalcopyrites is to form the alloys with MnTe, e.g. $(CuIn)_{1-z}Mn_{2z}Te_2$, and these alloys have been investigated in some detail [3–5].

Another group of compounds that show the tetrahedrally bonded form and contain Mn are the Mn–III_2–VI_4 compounds, e.g. $MnIn_2Te_4$, which have a defect $I\bar{4}2m$ tetragonal structure closely related to the $I\bar{4}2d$ structure of the chalcopyrites. These compounds have received some attention (e.g. [6,7]), but much less than the chalcopyrites, and recently alloy systems between these and the corresponding non-magnetic compounds, e.g. $CdIn_2Te_4$, have been studied [8–10]. For the alloy systems $Cd_{1-z}Mn_zGa_2Se_4$ [9], $Cd_{1-z}Mn_zIn_2Te_4$ [8] and $Zn_{1-z}Mn_zIn_2Te_4$ [10], in each case there is a change in space group symmetry of the terminal compounds from $I\bar{4}$ to $I\bar{4}2m$. However, in all three cases, single-phase solid solution occurs across the complete composition range for all temperatures below the solidus. The change in space group occurs in a very limited composition range and is observed only in terms of discontinuities in the various phase boundaries such as the solidus, etc. Corresponding discontinuities may occur in the variations of the lattice parameters and optical energy gap with z.

Because of the similarity of the two structures, it appeared probable that appreciable solid solution could occur between the chalcopyrite and Mn.III_2.VI_4 compounds, and the $T(z)$ phase diagram of the alloy system $Ag_{(1-z)}Mn_zIn_2Te_4$ has recently been investigated [11]. In addition to the different space groups of these two compounds, another difference in the cation arrangement is that while in the chalcopyrite-type $AgInTe_2$ the Ag and In atoms are fully ordered on the cation sublattice, in $MnIn_2Te_4$ the lattice vacancies are ordered on the cation sublattice but the Mn and In atoms

* Corresponding author. Permanent address: Physics Department, University of Ottawa, Ottawa, Ontario, Canada K1N 6N5.

SSDI 0925-8388(94)01511-2

occupy the remaining cation sites at random. In this system also, at temperatures just below the solidus there is complete solid solution for all values of z, in the form of a cation-disordered zincblende structure. However, when cation ordering occurs at lower temperatures, this results in an eutectoid reaction and gives a relatively wide miscibility gap between the single-phase fields corresponding to the terminal structures.

It has been shown [12] for these Mn.III$_2$.VI$_4$ compounds that those in which the Mn are disordered have very different magnetic behaviour from those showing an ordered Mn arrangement. These differences in magnetic behaviour are discussed in detail elsewhere.

In the present work, another of the mixed I.III.VI$_2$–Mn.III$_2$.VI$_4$ alloy systems, viz. $(CuInTe_2)_{2(1-z)}(MnIn_2Te_4)_z$, more conveniently labelled $Cu_{2(1-z)}Mn_zIn_2Te_4$, has been investigated, and the forms of the phase diagram and optical energy gap data compared with those of previous similar systems containing manganese.

2. Sample preparation and experimental measurements

Alloy samples of $Cu_{2(1-z)}Mn_zIn_2Te_4$ with various values of z were prepared by the usual melt and anneal technique. The components of each 1.0 g sample were sealed under vacuum in a quartz capsule, melted together at 1150 °C, annealed to equilibrium at 500 °C and very slowly cooled to room temperature. Previous experience indicates that for this type of alloy, this procedure gives samples showing conditions corresponding to equilibrium at 200–300 °C. Guinier X-ray powder photographs were used to check each sample and lattice parameter values were determined as a function of z, with germanium as internal standard.

Transition temperatures were determined from differential thermal analysis (DTA) measurements with silver used as reference material. The charge was of powdered alloy of typical weight 50–100 mg. The temperature of the sample and the reference were determined with chromel–alumel thermocouples, the difference signal between the sample and the reference and the temperature signal being continuously recorded. For each peak in the difference signal, a phase transition temperature was determined from the baseline intercept of the tangent to the leading edge of the peak [13]. Both heating and cooling runs were made, the average rates of heating and cooling being approximately 15 °C min^{-1}.

Slices of each single-phase sample were cut and thinned down to give specimens for optical absorption measurements by the usual method [14]. Values of $\ln(I_0/I)$, where I_0 and I are the incident and transmitted intensities, respectively, were determined as a function of photon energy $h\nu$ and corrected by subtracting a background value to give the absorption coefficient. Graphs of $(\alpha h\nu)^2$ vs. $h\nu$ were then used to give values of the optical energy gap E_0.

3. Experimental results and analysis

The X-ray photographs for the samples annealed at 500 °C showed the expected form, the alloys at the $CuInTe_2$ end of the diagram having the standard chalcopyrite structure α whereas the ones close to $MnIn_2Te_4$ had the form attributed to $I\bar{4}2m$ symmetry. A few alloys close to the centre of the diagram clearly showed both phases. Values of lattice parameters were determined in all cases and the variations of a and z are shown in Fig. 1, c/a being 2.00 in all cases. The probable error in the lattice parameter values was estimated to be ± 0.0005 nm. In the two single-phase regions, within the limits of experimental error, a varies linearly with z and from the a values in the two-phase region, the limits of single-phase solid solution were estimated to be $z = 0.37$ and 0.76. Straight-line fits to the two linear regions gave

$$a_\alpha = 0.6198 + 0.00122z \text{ (nm)} \qquad R = 0.992$$

$$a_\gamma = 0.6163 + 0.00363z \text{ (nm)} \qquad R = 0.985$$

DTA measurements were made on each sample and the resulting $T(z)$ diagram is shown in Fig. 2, the estimated relative accuracy of the points being ± 15 K. The two compounds show transition temperatures in agreement with those published previously [15,16]. Thus $CuInTe_2$ has the tetragonal chalcopyrite structure α up to 672 °C, above which it assumes the disordered zinc blends β structure, whereas $MnIn_2Te_4$ is tetragonal $I\bar{4}2m$ (γ) up to 630 °C, above which it also disorders

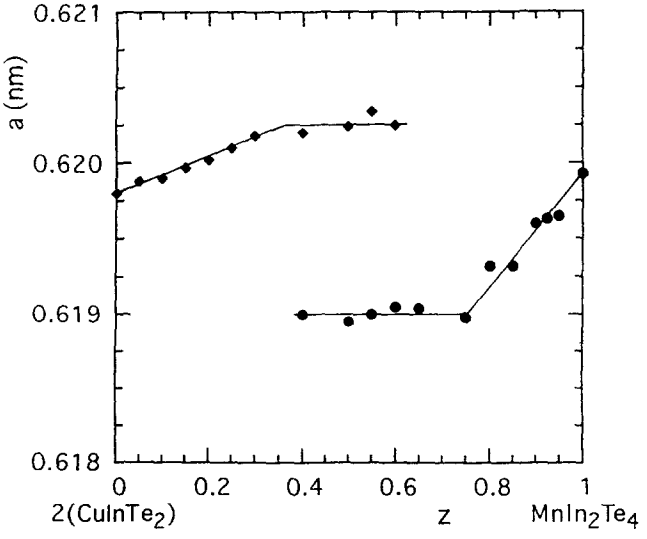

Fig. 1. Variation of lattice parameter a with composition z for the $Cu_{2(1-z)}Mn_zIn_2Te_4$ alloys. (●, ◆) Experimental values; (——) lines fitted to linear equations.

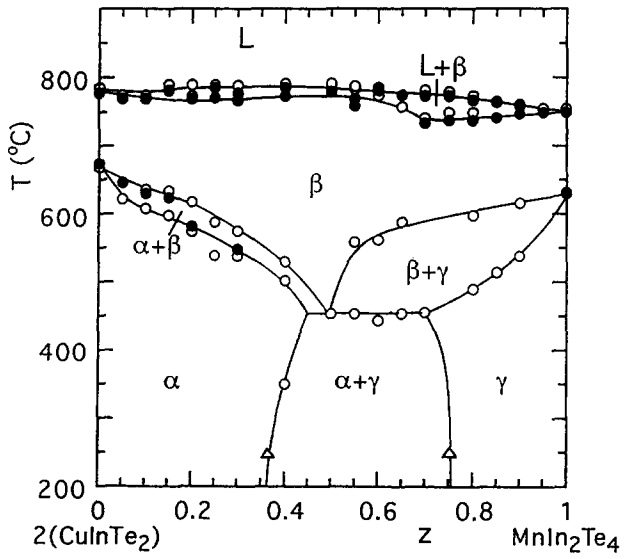

Fig. 2. $T(z)$ diagram for the $Cu_{2(1-z)}Mn_zIn_2Te_4$ alloys; (O) DTA heating run; (●) DTA cooling run; (△) value from lattice parameter data; (α) chalcopyrite $I\bar{4}2d$ structure; (β) disordered defect zinc blende structure; (γ) ordered tetragonal $I\bar{4}2m$ structure.

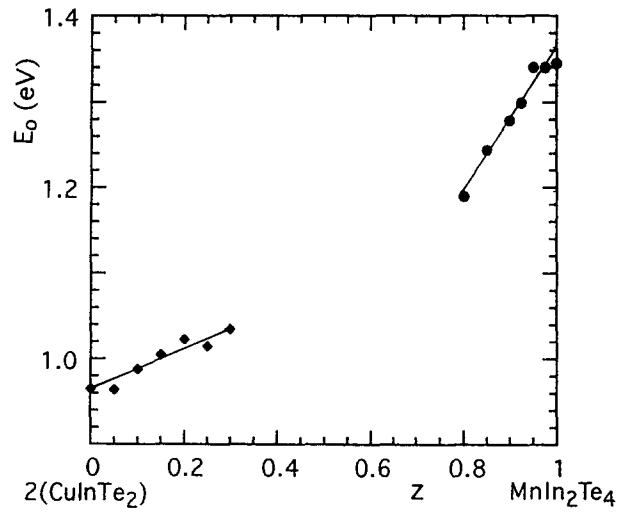

Fig. 3. Variation of optical energy gap E_0 with composition z for the $Cu_{2(1-z)}Mn_zIn_2Te_4$ alloys. (●, ♦) Experimental values; (—) lines fitted to linear equations.

to β. The zinc blende β phase thus extends across the complete diagram and disappears in a eutectoid reaction at $z=0.49$ and $T=452$ °C. Only one DTA point was observed below the eutectoid temperature, indicating that the phase boundaries were very steep. However, the boundaries representing the limits of the α and γ fields at about 200 °C were obtained from the X-ray data, as shown in Fig. 2. At any composition z for which a single-phase ordered structure (α or γ) was observed, between the two single-phase fields (α and β or γ and β), the heating curves clearly showed two transitions as seen in Fig. 2. In the previous diagrams considered above, this intermediate region was always interpreted as a two-phase field ($\alpha+\beta$ or $\beta+\gamma$) and, for convenience, the fields in Fig. 2 have been labelled in this way. However, it is possible that in certain cases a continuous transition can occur between the disordered and ordered phases rather than the two-phase behaviour mentioned above, as has been shown for the cases of $MnGa_2Te_4$ in the section $(MnTe)_{1-x}(Ga_2Te_3)_x$ [17] and $CuInSe_2$ in $(Cu_2Se)_x(In_2Se_3)_{1-x}$ [18]. Further detailed work is needed to determine the exact form of these fields in the various diagrams mentioned above.

Optical energy gap E_0 values were determined for all single-phase samples and the resulting variation of E_0 with z is given in Fig. 3. Within the limits of experimental error, E_0 varies linearly with z in both single-phase fields, although the slope of the E_0 vs. z line is different in the two cases. Straight-line fits to the data in the two regions yielded.

$$E_{0\alpha}=0.962+0.248z \text{ (eV)} \qquad R=0.960$$

$$E_{0\gamma}=0.547+0.814z \text{ (eV)} \qquad R=0.982$$

4. Discussion

As indicated in the Introduction, the limiting phases in this system are very similar; both are based on the zinc blende sub-cell and are ordered to give a tetragonal lattice with $c/a=2.00$. However, there is a change in space group, $CuInTe_2$ having $I\bar{4}2d$ symmetry and $MnIn_2Te_4$ being $I\bar{4}2m$. The very similar alloy system $Ag_{2(1-z)}Mn_zIn_2Te_4$ has been investigated recently [11] and also alloy systems containing Mn under similar conditions having the form $II_{1-z}.Mn_z.III_2.VI_4$, e.g. $Cd_{1-z}Mn_zIn_2Te_4$, [8–10]. In these latter cases, the space group changes from $I\bar{4}$ at $z=0$ to $I\bar{4}2m$ at $z=1$. It is of interest to compare the results for these various alloys with the present data.

For all three $II_{1-z}.Mn_z.III_2.VI_4$ systems, i.e. $Cd_{1-z}Mn_zGa_2Se_4$ [9], $Cd_{1-z}Mn_zIn_2Te_4$ [8] and $Zn_{1-z}Mn_zIn_2Te_4$ [10], at room temperature and above, a single-phase solid solution is found across the complete composition range; the change in space group (from α to γ) occurs at a particular composition, and results in a discontinuity in the phase boundary corresponding to the ordering temperature. Above this line, at $z=1$, the structure is the completely disordered zinc blende β phase, but at $z=0$, the structure is a partially ordered tetragonal form α'. The transition from α' to β occurs at the same composition as the α–γ transition and results in a discontinuity in the solidus curve. One alloy system has a similar discontinuity in the lattice parameter values, while another exhibits a discontinuity in E_0. No two-phase field has been observed at the change in space group, and if one occurs it will be very narrow in z.

In the cases of $Ag_{2(1-z)}Mn_zIn_2Te_4$ and the present system, the behaviour is different. The two phases (α and γ) of different space group are components in the

eutectoid reaction involving the zinc blende β phase, which extends across the complete diagram. A relatively wide two-phase ($\alpha+\gamma$) field occurs, and hence there are no boundary discontinuities to be observed. The variations in lattice parameters and optical energy gap with z are divided into two separate sections, and within experimental limits each section can be considered as linear.

Thus, as far as the $T(z)$ diagrams are concerned, although for the two different alloy combinations the differences in space groups appear comparable, the behaviour of the alloy systems is very different. A discussion, in terms of Landau's theory of second-order phase transitions [19,20], of the different behaviours of a number of systems which show this type of change in space group will be given elsewhere.

Acknowledgments

The authors are grateful to BID-CONICIT (project MN-09) and CDCHT-ULA for financial support. They thank Javier Ruiz for assistance with the preparation of the samples.

References

[1] J.K. Furdyna and J. Kossut, Diluted magnetic semiconductors, in *Semiconductors and Semimetals,* Vol. 25, Academic Press, New York, 1989, Chapter 1.

[2] Y. Shapira, E.J. McNiff, Jr., N.F. Oliveira, Jr., E.D. Honig, K. Dwight and A. Wold, *Phys. Rev. B, 37* (1988) 411.

[3] M. Quintero, E. Guerrero, P. Grima and J.C. Woolley, *J. Electrochem. Soc., 136* (1989) 1220.

[4] C. Neal, J.C. Woolley, R. Tovar and M. Quintero, *J. Phys. D, 22* (1989) 157.

[5] M. Quintero, R. Tovar, H. Dhesi and J.C. Woolley, *Phys. Status Solidi A, 115* (1989) 157.

[6] K.-J. Range and H.-J. Hübner, *Z. Naturforsch., Teil B, 31* (1976) 886.

[7] G. Delgado, C. Chacón, J.M. Delgado and V. Sagredo, *Phys. Status Solidi A, 134* (1992) 61.

[8] E. Guerrero, M. Quintero, M. Delgado and J.C. Woolley, *Phys. Status Solidi A, 115* (1992) K83.

[9] E. Guerrero, M. Quintero, R. Tovar, T. Tinoco, J. González and J.C. Woolley, *J. Electron Mater., 22* (1993) 297.

[10] M. Morocoima, M. Quintero and J.C. Woolley, *J. Solid State Chem.,* in press.

[11] R. Cadenas, M. Quintero and J.C. Woolley, *J. Solid State Chem.,* in press.

[12] J.C. Woolley, S. Bass, A.-M. Lamarche and G. Lamarche, *J. Magn. Magn. Mater., 131* (1994) 199.

[13] R. Chen and Y. Kirsh, *Analysis of Thermally Stimulated Processes, International Series Science of Solid State,* Vol. 15, Pergamon Press, Oxford, 1981, p. 97.

[14] R.G. Goodchild, O.H. Hughes, S.A. López-Rivera and J.C. Woolley, *Can. J. Phys., 60* (1982) 1096.

[15] L.S. Palatnik and E.I. Rogacheva, *Sov. Phys. Dokl., 12* (1967) 503.

[16] M. Quintero, M. Morocoima, E. Guerrero, R. Tovar, M. Delgado and J.C. Woolley, *J. Cryst. Growth, 114* (1991) 661.

[17] L. Garbato, A. Geddo-Lehmann, F. Ledda, M. Cannas and O. Devoto, *Jpn. J. Appl. Phys., 32* (1992) 389.

[18] J.C.W. Folmer and H.F. Franzen, *Phys. Rev. B, 29* (1984) 6261.

[19] L. Landau and F. Lifshitz, *Statistical Physics,* Pergamon Press, New York, 1959.

[20] H. Franzen, *Second Order Phase Transitions and the Irreducible Representation of Space Groups,* Vol. 32 of Lecture Notes in Chemistry (K. Ruedenberg et al., eds.), Springer, Heidelberg, 1982.